Faraday Discussions

Accepted Manuscript

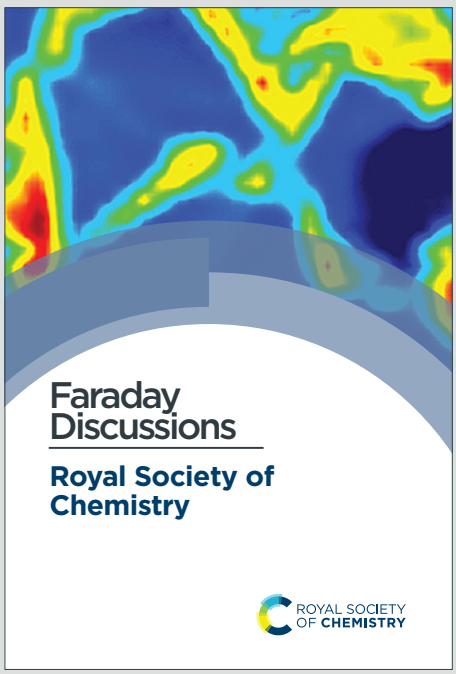

This article can be cited before page numbers have been issued, to do this please use: M. H. Godinho, R. Chagas, P. Silva, S. N. Fernandes and S. Zumer, *Faraday Discuss.*, 2020, DOI: 10.1039/D0FD00020E.

Playing the Blues, the Greens and the Reds with Cellulose-based Structural Colours

Ricardo Chagas,[a] Pedro E. S. Silva,[a] Susete N. Fernandes,[a] Slobodan Žumer[b, c] and Maria Helena Godinho[a]*

[a] i3N/CENIMAT, Department of Materials Science, NOVA School of Science and Technology, NOVA University Lisbon, Campus de Caparica, 2829-516 Caparica, Portugal.

[b]Jozef Stefan Institute, Jamova 39, 1000 Ljubljana, Slovenia.

[c]Faculty of Mathematics and Physics, University of Ljubljana, 1000 Ljubljana, Slovenia.

*corresponding author: mhg@fct.unl.pt

Abstract

Structural vivid colours can arise from the interference of light reflected from structures exhibiting periodicity on scales in the range of visible wavelengths. This effect is observed with light reflected from cell-walls of some plants and exoskeletons of certain insects. Sometimes the colour sequence observed for these structures consists of nearly circular concentric rings that vary in colour from Red, Orange, Yellow, Green, Cyan and Blue, from the periphery to the centre, similarly to the sequence colour scheme observed for the rainbow (ROYGB). The sequence of colours has been found for solid films obtained from droplets of aqueous cellulose nanocrystals (CNCs) solutions and attributed to a "coffee ring" effect[1-4]. In this work, coloured lyotropic solutions and solid films obtained from a cellulose derivative in the presence of trifluoroacetic acid (TFA), which acts as a "reactive solvent", are revisited. The systems were investigated with spectroscopy, using circularly and linearly polarised light, coupled with a polarised optical microscope (POM) and scanning electron microscopy (SEM). The lyotropic cholesteric liquid crystalline solutions were confined in capillaries to simplify 1D molecular diffusion along the capillary where an unexpected sequence of the structural colours was observed. The development and reappearance of the sequence of vivid colours seem consistent with the reaction-diffusion of the "reactive solvent" in the presence of the cellulosic chains. The strong TFA acts as an auto-catalyst for the chemical reaction between TFA and the hydroxyl groups, existing along the cellulosic chain, and diffuses to the top and bottom along the capillaries, carrying dissolved cellulosic chains. Uncovering the precise mechanism of colour sequence and evolution in time in cellulosic lyotropic solutions has important implications for future optical/sensors applications and for the understanding of the development of cellulose-based structures in nature.

View Article Online
DOI: 10.1039/D0FD00020E

Introduction

Structural colours are present in animals and plants forming different patterns. For instance, in peacock feathers (Fig. 1 a.), the eyespots developed on the feather of the adults present a repetition of colours, along the radius of the eyespot, that goes from the blue at the centre to green, bronze, green, bronze, green at the periphery[5, 6]. The formation of the colours of the eyespot comprises different stages that appear progressively, starting with the appearance of a dark brown at the middle, in young peacocks, changing to the sequence of vivid colours that are observed in the adult eyespot. The formation of the colours in the eyespots evolves over approximately 3 years[6]. Other designs involve the sequence of concentric coloured circles, which are blue, green and red from the centre to the periphery as the spots observed on *Pachyrrhynchus congestus pavonius*[7] (Fig. 1 b). Reaction-diffusion models were suggested to describe the pattern formation of the eyespot[8] as well as the spots exhibited by the *Pachyrrhynchus congestus pavonius spots*[9].

Structural colouration can also arise by the presence of cholesteric-like liquid crystal structures consisting of uniform natural twisted arrangements of anisotropic entities around a normal axis (optical axis). The vivid colours of the exoskeletons of some beetles (example of *C. aurata* are one of the many examples of the role of nature's existing helical structures[10, 11]. Cholesteric structures were also found in cellulose-based systems. Actually, the structural colours present in cellulosics are due to cholesteric phases that are obtained from lyotropic and/or thermotropic systems that were much studied in the eighties[12-18]. After the preliminary studies many other works were performed in order to obtain different coloured thermotropic cellulose derivatives, at room temperature, and to better understand the formation of right- and left-handedness in cellulose-based helicoidal liquid crystalline phases[19-26]. The photonic characteristics of the thermotropic, as well as lyotropic cellulosic systems, were found to depend on temperature, pressure, concentration, type of solvent and cellulose derivative. The substituent, the average number of cellulose hydroxyl groups substituted per anhydro glucose unit, degree of substitution ($\overline{\mathrm{DS}}$), and the average molecular weight of the cellulose derivative were found to be crucial factors that influence not only the value of the cholesteric pitch but also the handedness of the helical structure[23, 24]. One of the first thermotropic cellulose derivatives to be synthesized was acetoxypropylcellulose (APC), which exhibits liquid crystalline behaviour at room temperature. The temperature to the isotropic phase was found to increase with the value of the $\overline{\mathrm{DS}}$ of the polymer. The rotations about glycosidic bonds are hindered

in the cellulose backbone being the stiffness of the polymer affected by a high degree of acetyl content[18, 26]. Several other thermotropic esters such as propionic, butyric, isobutyric, valeric, isovaleric, hex- and heptanionic acid esters of hydroxypropylcellulose (HPC), with different side-chain lengths were reported in the literature[19]. It was highlighted that the values of the cholesteric pitch vary with the length of the side-chain substituent as well as with temperature[19].

In addition to these factors it was also reported in the literature the inversion of chirality of the cholesteric phase for cellulose derivatives, which occurs not only for thermotropic[24] but also for lyotropic systems[23]. The tri-o-(β-methoxyethoxy)ethyl cellulose, with a degree of polymerization ($\overline{\mathrm{DP}}$) of 11, was the first reported thermotropic cellulose derivative, which presented chirality inversion with temperature[24]. The effect observed was discussed in terms of the twist imposed by the asymmetric carbons existing along the cellulose main chain, which competed with the formation of an opposite sense helical polymer conformation induced by the presence of the side-chains[24].

In solution, varying the values of the $\overline{\mathrm{DS}}$ of the polymer may also induce the reversal of the cholesteric handedness by passing the system through a nematic phase (P = ∞)[25].

One of the examples is a lyotropic cholesteric system well described in literature prepared from acetyl-ethyl-cellulose (AEC) with the same value of the $\overline{\mathrm{DS}}$ of ethyl and different values of the $\overline{\mathrm{DS}}$ of acetyl groups. The AEC derivatives were found to form lyotropic solutions, in a great variety of organic solvents, which showed a handedness inversion, with the acetyl content of the polymer. At a given degree of acetylation of the polymer, which the authors named compensated degree of acetylation, the mesophase became nematic and the pitch infinite[24]. In order to denote the orientation of the cellulose semi-rigid macromolecules (rods), at a given point of the liquid crystalline solution, a unit vector, **n**, named director was used and the degree of order, $S = \frac{1}{2}\langle 3\cos^2\theta - 1\rangle$, where θ specifies the angle that the rods make with the director and the brackets represent the ensemble average, was calculated and for hydroxypropyl cellulose and ethyl cellulose solutions the values of S were found to be of the order of 0.4-0.8[27].

The optical properties of cellulose acetate cholesteric liquid crystals in trifluoroacetic acid (TFA) were also investigated and in the presence of the strong acid the cellulose diacetate forms a left-handed cholesteric phase, for a given initial TFA concentration. The pitch increases in time evolving to a right-handed phase. The increasing of the pitch with time was attributed to a self-catalysed esterification reaction that occurs between the carboxylic acid and the free hydroxyl groups of the cellulose acetate backbone[17].

However, the topic is not closed and recently thermotropic mixed esters of hydroxypropylcellulose (HPC), with butyryl and fluorobutyryl substituents, were synthesized[27]. The pitch of the cholesteric structure was found to be very sensitive to the fluor substituent. A low average degree of substitution ($\overline{DS}$ of the order of 0.15), of the fluor moiety, translated into a significant increase of the pitch value, compared with the pitch for the thermotropic with only butyryl substituents. The mixed esters presented selective reflection of RCP light and vivid colours from violet to red depending on the $\overline{DS}$ of the substituents and on temperature [28].

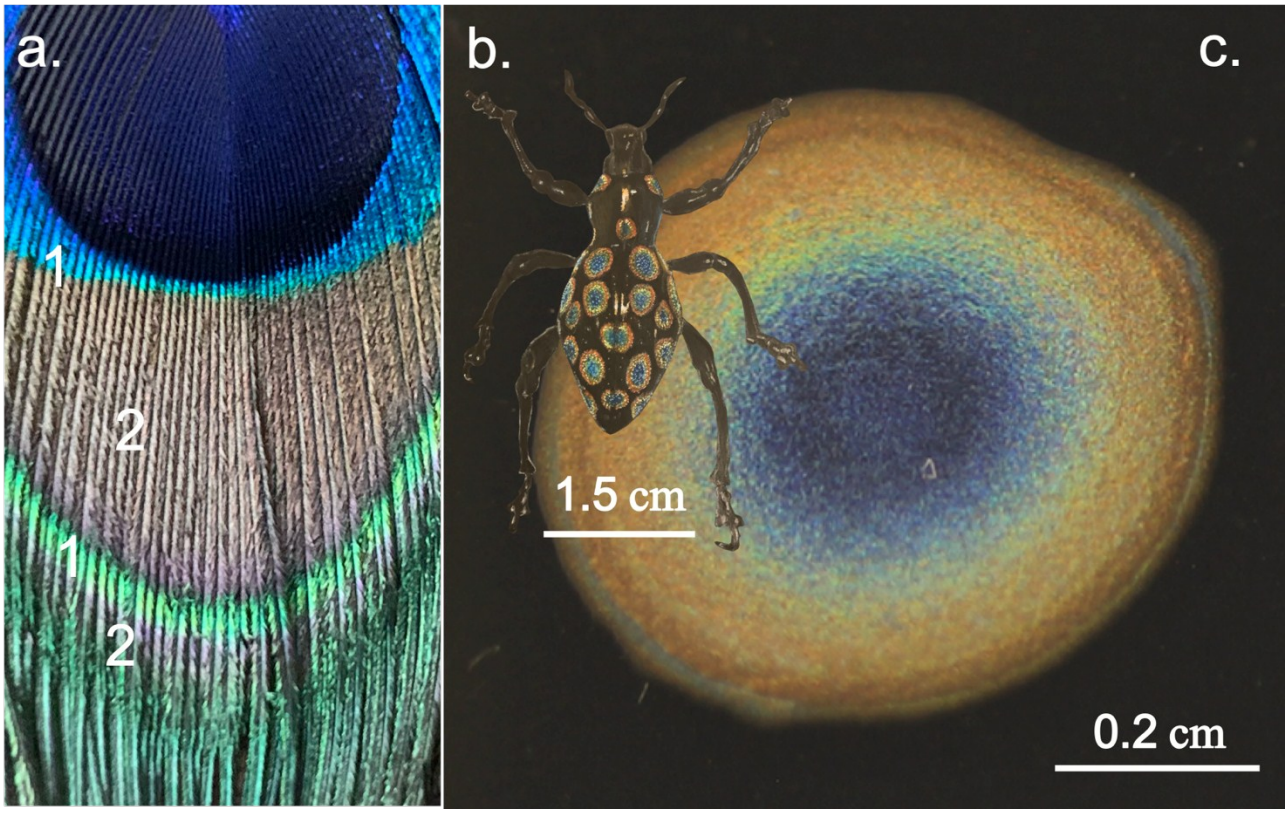

Figure 1. a. Detail of a peacock feather with blue, green, yellow and brown barbules sticking out from a common shaft. The green (1) and brown (2) colours are marked as examples of colours that repeat from the centre to the periphery. b. *Pachyrrhynchus congestus* weevils drawing (pencil on black paper), showing rainbow spots similar to the "coffee ring" effect exhibited by a film casted from a droplet of cellulose nanocrystals (CNCs) suspension, shown in c. The photos were taken under uncollimated unpolarized white light.

Moreover, it has been reported in literature a sequence of colours, ranging from red to blue, such as in the rainbow, in thin solid films prepared from droplets of anisotropic cellulose nanocrystals (CNCs) aqueous solutions, after solvent evaporation. The appearance of the rainbow at the periphery of the circular films was attributed to the existence of a "coffee ring" effect[1-4] (Fig. 1 c.).

In this work we use micro spectrophotometry, polarised light optical microscopy (POM) (reflection and transmission) and scanning electron microscopy (SEM) to study a cellulosic lyotropic cholesteric

system, which presents an unusual sequence of colouration in time. For the first time a decrease followed by an increase of reflected vivid colours observed in lyotropic cellulosic systems is reported. A reaction-diffusion mechanism, due to the presence of the strong acid that acts as "solvent", is suggested to explain the unusual sequence of the structural colours observed in time.

Experimental

Materials and Methods

Solutions Preparation:

Cholesteric liquid crystalline solutions of (hydroxypropyl)methyl cellulose (HPMC, Methocel F50, Dow, Average Molecular Weight in Number 20-25 KDa) in trifluoracetic acid (TFA, ReagentPlus, 99% purity, Sigma Aldrich), 20% w/w (C_A) and 23% w/w (C_B), with reflection bands in the visible region, were obtained by direct mixing in glass vials with a needle, which were sealed with a cap after preparation of the samples and left to homogenise at 4 ^oC. After approximately 24 hours, iridescent solutions were obtained and stored at 4 ^oC until further use (Fig. 2).

Characterization:

Scanning electron microscopy (SEM) Observation:

The cross-section of the solid films was observed by SEM, at room temperature. A Carl Zeiss Auriga crossbeam (SEM– focus-ion-beam (FIB)) workstation instrument, equipped with an Oxford energy-dispersive X-ray spectrometer, was used to obtain the SEM images. Samples were mounted in aluminum stubs, coated with a thin carbon layer using a Q150T ES Quorum sputter coater. The acquisition was performed using an accelerating voltage of 2 or 5 kV with 5.6–7.2 mm as working distance.

Hue-Value Diagrams: Images were first converted from the RGB (red, green and blue) colour space to HSV colour space (hue, saturation and value)[29]. Next, colour averages were clustered by using the k-means method. When compared with methods that partition the colour space equally, the k-means method allows the identification of colour variability with a smaller number of bins[30]. We found that using ten clusters were enough to capture colour distribution for a single image. For representing all images averages in a single diagram, only one cluster centre was calculated.

Spectroscopy, Photographs, Videos, and Optical Images:

Photographs of the solutions in the vials and capillaries were obtained with a Canon EOS 550D coupled with an EF-S 60 mm Canon macro-lens under visible light. Microscopy optical images were obtained in reflection mode, by using an Olympus BX51 microscope, coupled with an Olympus DP73

CCD camera, and acquired with the Stream Basic v.1.9 Olympus software. A cold illumination source generated by a halogen lamp (KL 2500 LCD, SCHOTT) was used. The images were obtained with ×20 objective (Olympus, MPlanFL N) and automatically scaled by the software. The reflective wavelengths detected with cross polarizers were recorded with a Sense+Sarspec VIS spectrometer, mounted onto the microscope, and acquired with the LightScan 1.1.17 software. Each reflectance spectrum was normalized to the maximum registered value. Measurements as a function of temperature were obtained by placing the samples in a hot stage Mettler FO82HT, coupled with a control processor Mettler F90, with an accuracy of 0.1°C at 2°C/min and fixed on the microscope stage. The samples were heated at a rate of 2°C/min. The wavelength values (λ) reflected by the samples vary with the pitch (P) of the cholesteric phase according to the de Vries equation, $\lambda = \bar{n}P \sin\theta$[31], being $\bar{n}$ the average refraction index of the material and θ the angle between the incident light and the plane of the cholesteric layers. If the material is illuminated parallel to the optical axis ($\theta = \frac{\pi}{2}$), the maximum wavelength, λ_0, of the reflection peak is given by, $\lambda_0 = \bar{n}P$, and the width at half maximum (FWHM), $\Delta\lambda$, is related to the birefringence, Δn, according to, $\Delta\lambda = \Delta n P$. The values $\bar{n}$, and Δn are, for cholesteric liquid crystalline phases of cellulose derivatives, of the order of 1.4 and 0.003, respectively[13].

Chemical characterization via Fourier Transform Infrared (FTIR) spectroscopy was performed on the initial HPMC sample and on the polymer collected from a solution 4 days after capillaries preparation FTIR spectra of the samples were recorded on a Perkin-Elmer FTIR Spectrometer Spectrum Two (Waltham, MA, USA), equipped with an attenuated total reflection cell (ATR), in the range of 4000– 400 cm^{-1} with a 0.5 cm^{-1} resolution (Sup. Mat. Fig. S4).

View Article Online
DOI: 10.1039/D0FD00020E

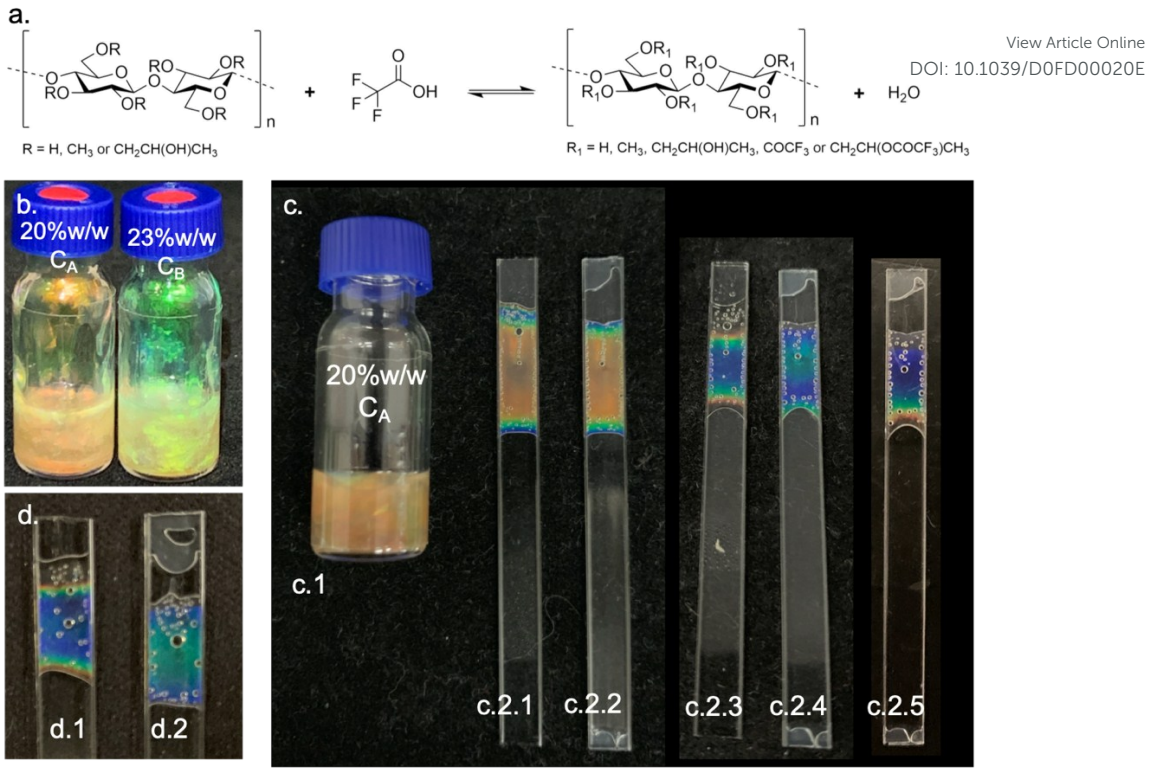

Figure 2. Lyotropic cellulosic system, hydroxypropylmethylcellulose (HPMC) in the presence of a "reactive solvent", trifluoracetic acid (TFA). a. Equilibrium chemical reaction of the esterification of HPMC in the presence of TFA. b. Cholesteric iridescent HPMC/TFA solutions, C_A=20% w/w and C_B=23% w/w (polymer weight/weight of solution). c. Evolution of C_A (c.1) solution in time, confined in an open, c.2.1, and a sealed, c.2.2, capillary, one hour after filling the capillary. c.2.3 and c.2.4 are c.2.1 and c.2.2, one day after and c.2.5 is c.2.4, after 2 days. d. Open (d.1) and sealed (d.2) capillaries prepared from C_B, one day after filling the capillaries. Capillaries dimensions; thickness 0.4 mm, width 4.0 mm. The diameter of the vials is 1.0 cm.

Solid films preparation:

Solid films were obtained from solutions prepared, 4 days after sample preparation, as thin layers between two microscope glass plates, followed by freezing, quenching and drying. The HPMC/TFA solution (30 µL) was placed between two glass plates. The solutions were allowed to relax until iridescence reapers in the microscopic preparations, at 25 °C. After 4 days the glass slides were put in liquid nitrogen to freeze the polymer structure. The quenching was achieved by removing the preparation from liquid nitrogen and dipping in ethanol. After 5 minutes, solid films were detached from the glass plates and washed in ethanol to remove the remaining TFA and other reactants and products soluble in the alcohol. The films were removed from ethanol and were dried under vacuum to remove residual ethanol. The obtained films were stored in a desiccator to avoid hydration.

Capillary filling:

The Glass capillaries (rectangle boro tubing 50 mm (length) × 4 mm (width) x 0.4 mm (thickness) path length, VitroTubes™) were filled with different HPMC/TFA solutions by using a syringe (Braun

disposable Injekt™, 1 mL) with a stainless-steel dosing needle (Itec, ½", 30 gauge). Petrolatum was used as the sealing agent for the capillaries. The optical axis of the cholesteric samples is perpendicular to the walls of the capillary except close to the air interfaces.

Results and discussion

The increase of the pitch of a cholesteric phase obtained from a cellulose derivative in the presence of trifluoracetic acid (TFA), as "reactive solvent", was reported in the literature[17]. TFA acts not only as a "reactive solvent" but also as a catalyst for an esterification reaction, which occurs between the free hydroxyl groups of the cellulose derivative and the carboxylic acid of TFA originating a cellulose ester and water (Fig.2a. and IR spectra (Suppl. Material)). In this work, we focus on the unusual evolution of the optical properties of the cholesteric lyotropic system, hydroxypropylmethyl cellulose (HPMC)/TFA (phase diagram in Sup. Mat. S1) in time: a decreasing of the pitch value in an initial stage followed by an increase of the pitch. The main emphasis is given to the sequence inversion of the colours and their development in samples enclosed in thin capillaries. Two cholesteric solutions were prepared from different initial concentrations of HPMC in TFA (C_A = 20% w/w and C_B= 23% w/w (weight of HPMC/weight of solution) (Fig.2b.). The initial C_A and C_B solutions present vivid iridescent colours, at room temperature. The maximum wavelengths, λ_0, reflected by the samples vary not only with concentration but also with temperature. As the temperature and the solvent concentration increase the pitch increases (Fig.3a. and 3.b). This type of behaviour is described and usually reported in the literature for lyotropic systems obtained from cellulose derivatives[12, 32]. However, the existence of two regimes is clearly seen for the variation of the pitch with temperature (see example in Figure 3 b. (C_B) and Sup. Mat. S2, Fig.S2), below and above a temperature around 312-314 K, where the slope of the curve's changes from 1.8 to 3.6 nm.K^{-1}, respectively.

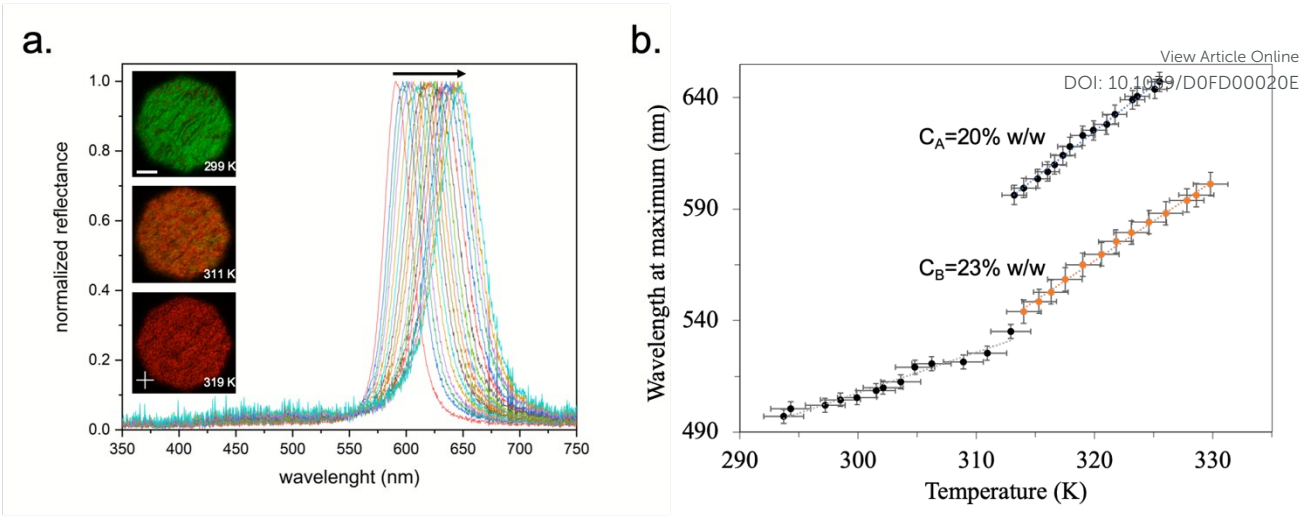

Figure 3. Variation of the pitch with temperature and concentration a. dependence of the wavelength reflected by C_A=20% w/w sample with temperature (the arrow indicates increasing temperature), the images on the left correspond to POM pictures taken in reflection mode between cross polarizers, for three different temperatures. b. dependence of the maximum wavelength with temperature and concentration for C_A and C_B. The spectra were taken at the same point at the centre of sealed samples, the first spectrum was acquired 5 minutes after sample preparation, heating rate 2°C/min. Scale bar 100 µm.

To investigate the development of the two regimes C_A and C_B solutions were further investigated inside the capillaries, which limit the typical time of 1D molecular diffusion along the distance l,$t_{mol} = l^2/2D$[33], being D the diffusivity coefficient, of the order of 10^{-7}-10^{-8} cm^2 s^{-1}, and $l \approx 16$ mm. The capillaries prepared from C_A (Fig.2c.) and C_B (Fig.2.d.) solutions show, some minutes after preparation and under white light illumination, a colour gradient, from the centre to the border of the capillary, with colours ranging from dark blue at the periphery of the sample to red, for C_A, and to blue, for C_B, at the centre (see supplementary material .gif animation). The sequence of the colours can be attributed to evaporation of the TFA from the menisci at the edges of the samples. This evaporation is necessarily accompanied by diffusion of TFA from the centre toward the edges of the sample. This effect is responsible for the shifting of the pitch to lower values at the periphery of the preparation.

To investigate the effect of TFA evaporation open and sealed capillaries were prepared from C_A (Fig.2 c.2.1 and c.2.2) and C_B (Fig.2 d.1 and d.2). One could expect the variation of the pitch in space and time should be monotonic if colours would depend only on the concentration of the evaporating solvent. This is true only at the beginning of observations, see capillaries in Fig.2. c.2.1 to c.2.3 and from c.2.2 to c.2.5. The encapsulated samples effectively evolve to a bright rainbowlike at the edges, with colours ranging from red at the border to dark blue in an inner stripe that spreads through the centre of the preparation. However, when the blue colouration, at the centre of the sample,

becomes green, then red, then surprisingly, a new rainbow begins to form at the border of the sample. The samples that were sealed display the same behaviour but delayed in time. The following observations deserve to be highlighted: a) the colour of the solutions, when transferred from the vials to the capillaries, is not the same as that observed in the vials. This is, at the centre of the capillaries, the wavelength, reflected by the samples, at normal incidence, is always shorter than that presented in the vials; b) the sealed capillaries show the same behaviour as the closed ones but for longer times; c) near the walls of the capillaries no coloured gradient is observed; d) two regimes could be identified, first the pitch of the solutions decreases (regime 1) from the centre to the periphery and then increases (regime 2). This behaviour is different from that described by Gray et al. for the lyotropic cellulose acetate/TFA lyotropic system, for which the value of the pitch was found to increase in time[17].

To precisely follow the behaviour of the solutions in regime 1, reflectance spectra were obtained for sealed capillaries prepared from C_A and C_B, near the border of the samples, and two hours after the preparation of sealed capillaries (Fig.4 a. and d. and the insets show the border of the capillaries). The samples were observed parallel to the optical axis of the cholesteric, C_A and C_B samples show values of the maximum wavelength, λ_0, of the reflectance peaks, that increases from the periphery to the centre of the sample. The initial concentration of the solvent, present in the lyotropic solution, determines the value of λ_0 at the centre of the sample. Since C_A is more concentrated in solvent the values of the pitch are higher than the values of the pitch measured for sample C_B. The POM images, taken in reflection mode, between cross polars (Fig. 4 b. and e.), and the reflectance spectra show that the sequence of colours from the border to the centre is blue, green, red for C_A and blue, green for C_B. The gradient of the colours indicates that the pitch decreases at the border, for both samples. Hue, saturation and value (HSV) colour diagrams (Fig.4 b. and d.) of C_A and C_B solutions were also recorded from the periphery to the centre of the sample, regions A to B in Fig.4 a. and c., respectively, between cross polars. The colour diagrams show, in polar coordinates, the variation of hue (angle) with value (radius). Each point corresponds to the average colour of each polarised optical microscopy (POM) image (Fig.4 b. and e. and Sup. Mat. S5, gif. animations). The behaviour observed can be attributed to the diffusion of TFA from the centre to the periphery, as observed for cellulosic lyotropic systems, when the solvent evaporates from the edges of the preparation.

However, let us remind that TFA also reacts with HPMC so that when its concentration is lowered due to evaporation and diffusion processes, the equilibrium of the chemical reaction (Fig.2 a.) will be shifted toward the formation of HPMC, less substituted than HPMC-$OCOCF_3$.

Knowing that the pitch decreases when the degree of substitution is lowered the initial rainbow-like colour sequence is reversed at edges of samples in the regime 2.

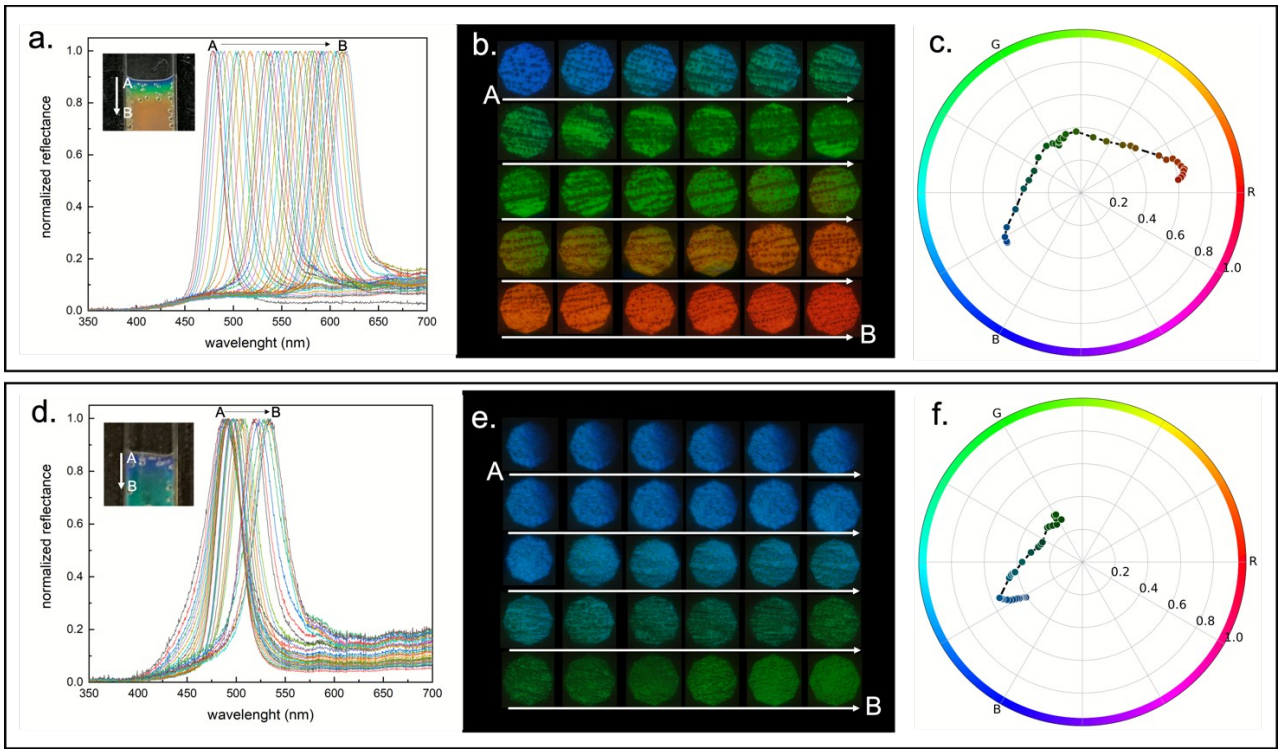

Figure 4. Colour evolution, at the border of the sample, of C_A and C_B lyotropic samples, confined in sealed capillaries, 2 hours after filling. a. and d. Reflectance spectra of C_A and C_B solutions, respectively recorded from region A to B (insets in a. and d.), between cross polars. b. and e. POM images were taken in reflection mode between cross polars, the images were recorded following the direction of the arrows from A to B, along the centre of the capillary. c. and f. HSV colour diagrams of C_A and C_B solutions, respectively, recorded from regions A to B, between cross polars. Colour diagrams show, in polar coordinates, the variation of hue (angle) with value (radius). Each point corresponds to the average colour of each POM image.

To highlight regime 2 the same sample, C_A, in figure 5, was followed in time. Two distinct behaviours are depicted. While for regime 1 (Fig.5 a.), as described before (2 hours after sample preparation) the pitch decreases from the centre to the periphery. For regime 2 (Fig.5 b.), sample C_A, shows a decrease of the pitch followed by an increase from the border to the centre of the sample. Since the sample is not centred at the middle of the sealed capillary, it is observed an asymmetry in the solvent evaporation, which largely occurs in the part of the capillary with most available space. This is evidenced by the development of different colours at the two borders of the same sample. The evolution of the colour to the red, at the periphery of the sample, is delayed if the evaporation of the "reactive solvent" is prevented.

In regime 2, the area occupied by the red colour, at the centre of the sample, reduces while a new red colour develops at the periphery. The green and blue colours expand between the two regions with red colour (Fig.5 b.).

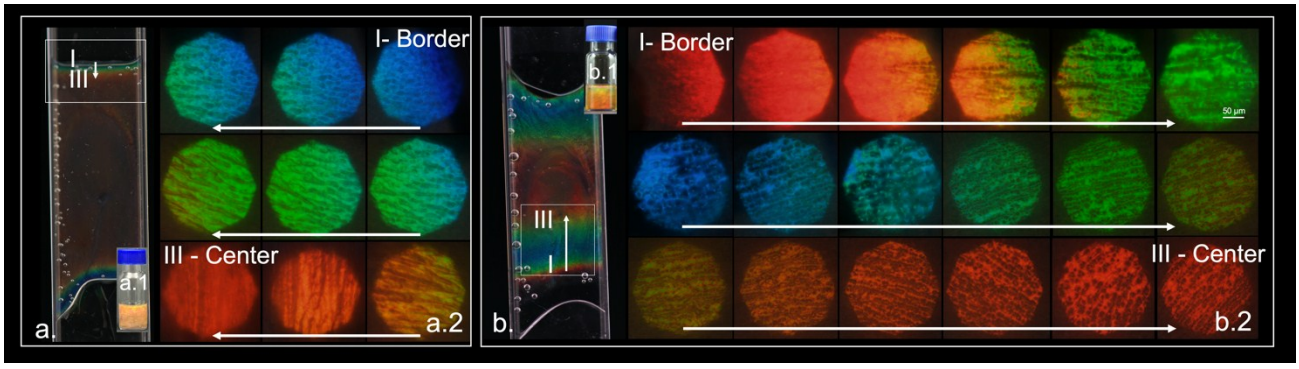

Figure 5. Time evolution of solution C_A (a.1). a. sealed capillary after one hour of sample preparation. a.2 optical microscopy images taken in reflection mode, between cross polars, from I to III (indicated in a.). b. capillary prepared from b.1, 2 days after sample preparation. b.2 optical microscopy images taken in reflection mode, between cross polars, from I to III (indicated in b.). The direction of the arrows in a.2 and b.2 correspond to the direction of the arrows indicated in a. and b., respectively. Capillaries dimensions; thickness 0.4 mm, width 4.0 mm. Diameter of the vials 1 cm.

For sealed capillaries, the menisci closer to the edge have a slower evolution than to the menisci farther to the edge of the capillary. This indicates that TFA diffuses at a slower rate at the shorter side of the capillary, which leads to symmetry breaking and fast reappearance of colours at the fast diffusion side (Fig. 2 c.2.2, c.2.4 and c.2.5). This symmetry breaking also indicates that the sealing agent only retards the process compared to the open capillaries but do not avoid, for a longer time, the diffusion of TFA.

To follow the evolution of the colour at the border and sketch a picture of the process involved, an encapsulated sample in a “sealed” capillary, with the meniscus more distant from the edge, was investigated (Fig.6). At the beginning, the sequence of colours observed follows a typical evaporation of a solvent with a higher concentration of the solvent at the centre. The sample is more concentrated in polymer at the periphery implying that a blue colouration appears near the meniscus (Fig.6 a.). Below the meniscus the cholesteric phase order from lower to higher TFA concentration corresponding to layers with different values of the pitch, as shown schematically in Fig.6 b.

The main difference between the lyotropic system TFA/cellulosic, described in this work, and other cellulose based lyotropic systems is that after this first stage, even if the solvent continues to diffuse from the centre, the sequence of colours reverses (Fig.6 c. and e. and graph Supp. Materials). This

unexpected behaviour can be explained considering the chemical reaction that exists between the cellulosic side hydroxyl groups and the carboxylic acid that becomes unstable due to the presence of diffusion. The evolution of the cholesteric layers, with different values of the pitch, is sketched in Fig.6 d. and 6 f.

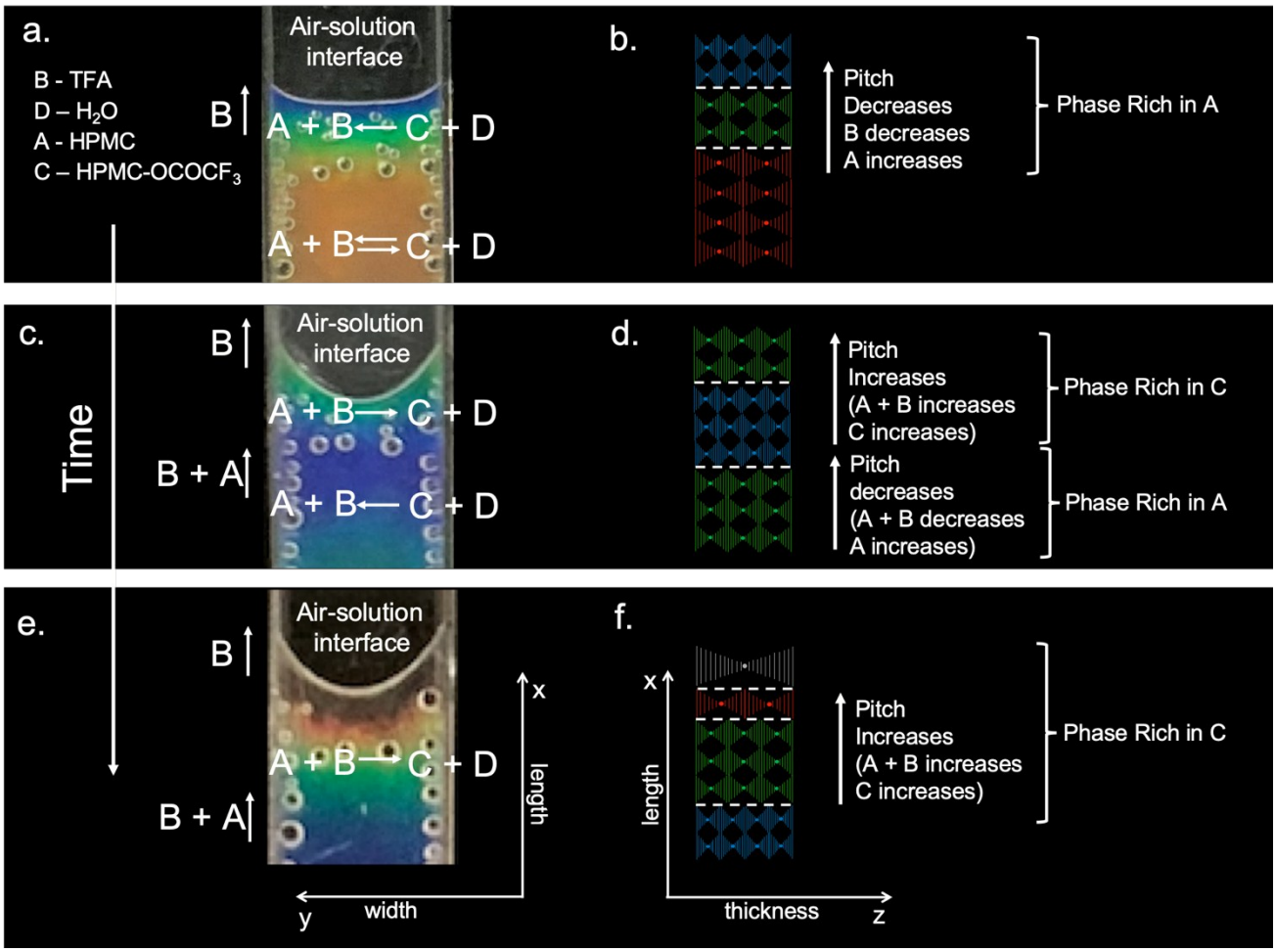

Figure 6. Chemical reactions and diffusion processes, in time, that might account for the development of coloured striped patterns of HPMC/TFA cholesteric solutions. a., c. and e. border of a sample confined in a closed capillary, seen along the main axis (x) and the width (y) of the capillary, 1 hour, 1 day and 2 days, respectively, after filling the capillary. The arrows pointing up indicates the diffusion of TFA and TFA+HPMC. The chemical reactions with the equilibrium shift to the formation of HPMC+TFA and HPMC-$OCOCF_3$+H_2O are indicated in the capillaries. b., d. and f. are schemes of the cholesteric structures, along the main axis (x) and thickness (z) of the capillary, that change in time as TFA diffuses and the chemical equilibrium is shifted. Capillaries in a., c. and e. are the same as in Figure 2 c.2.2, c.2.4 and c.2.5, the border of the sample observed is the furthest from the periphery of the capillary. The change of the meniscus curvature indicates a large change in the surface tension.

SEM images (Fig.7) show the top surface and the cross-section of solid films obtained from HPMC/TFA lyotropic solutions two hours after preparation of the solutions. The layered structure is indicative that the cholesteric structure, exhibited by the lyotropic solutions, was imprinted in the solid films. The micro/nano alveolate structure clearly observed at the top surface can be

understood as a fingerprint of the phase poor in HPMC-$OCOCH_3$ that was dissolved in ethanol, when the films were prepared. The morphology of the solid films seems to indicate not only the existence of a cholesteric structure but also the co-existence of two phases in the precursor lyotropic system.

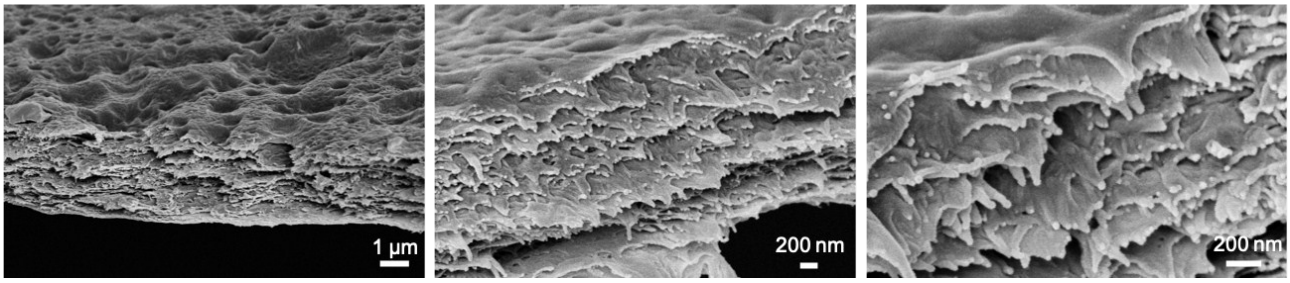

Figure 7. Scanning electron microscopy (SEM) images showing layered solid films with a top surface spotted with micron and nano alveolates, obtained from HPMC/HPMC-$OCOCF_3$/TFA lyotropic solutions, rich in HPMC.

A possible explanation of the results obtained can be as follow: TFA acts as a solvent for HPMC, forming a lyotropic phase, above a certain critical concentration. It is also a reactant and a catalyst for the esterification reaction that occurs between the side free hydroxyl groups of HPMC and the trifluoro carboxylic acid, according to the equilibrium equation: $\mathrm{A} + \mathrm{B} \rightleftarrows \mathrm{C} + D$ (I), where the reactants are A – HPMC and B – TFA and the products C – HPMC-$OCOCF_3$ and D – H_2O, (according to Fig.2a. and Fig.6). TFA is a very volatile solvent (surface tension, 1,4 $x10^{-2}$N/m) with a boiling point of 72°C that can easily diffuse from inside of the capillaries to outside. The diffusion of TFA and its role on the optical properties of the system is confirmed by the use of open and closed capillaries. When the capillaries are closed, and the sample placed asymmetrically, the development of the sequences of colours is delayed for the short side of the capillary (see for example Fig.2 c2.4) when compared to the open capillaries (Fig.2 c2.3 and c2.4). Thus, the diffusion of TFA, from the centre of the solution to the border of the capillaries, starts the whole process. The TFA diffusion promotes a concentration gradient and shifts the equilibrium of the chemical reaction towards the formation of A. The first decrease of the pitch, which was observed at the border and at the centre of the samples can be attributed to the initial diffusion of TFA. However, as TFA diffuses to the periphery of the capillaries it carries dissolved molecules of the polymer, which increases the viscosity of the fluid and retains more A+B at the border of the sample. The increase of A at the border shifts the chemical equilibrium to the formation of C. This implies, near the border, a phase richer in C and at the centre a phase richer in A. As described in literature the value of the pitch increases with the degree of substitution for some cellulose derivatives[17, 18, 21] and for the lyotropic system under study (see Sup.

Mat. S2, Fig. S3), since C is more substituted than A the value of the pitch increases at the periphery of the sample. In time, the continuous diffusion of A+B, from the centre to the border, always shifts the equilibrium towards the formation of A at the centre and the formation of C at the border increasing the pitch of the sample, as the concentration of C increases, from the border to the centre. The processes of diffusion, and of shifting the equilibrium of the chemical reaction remain continuously until HPMC-OH is consumed (the evolution of the curvature of the meniscus indicates a variation of the surface tension, which is an indication of the chemical reaction).

Considering the coloured striped patterns obtained, perpendicular to the main axis of the capillaries, an activator–inhibitor model can be suggested. The diffusion of the trifluoroacetic acid along the main axis of the capillaries (x direction) seems to be crucial to the development of the coloured stripes. Diffusion tends to make the concentration uniform in the system. However, in the studied lyotropic cellulose-based/TFA system gradients in concentration seem to arise in the presence of the chemical reaction and diffusion. One of the necessary conditions for the development of spatial patterns implies the existence of an activator and an inhibitor. The value of the reaction rate should increase with concentration for the activator and the reaction rate of the inhibitor should decrease as the concentration increases. Another necessary condition, for the development of spatial patterns, is[35]: $\frac{D_{inhibitor}}{D_{activator}} > 1$, being $D_{inhibitor}$ and $D_{activator}$ the diffusion rate constants of the inhibitor and activator, respectively. In the present study the inhibitor would be the trifluoroacetic acid, which diffuses faster than the HPMC molecules, $\frac{D_{[COOH]}}{D_{[OH]}} > 1$, decreasing the concentration of TFA implies that the rate of the reaction towards the formation of HPMC-OH molecules increases. These characteristics of the system may be at the genesis of the observed patterns, which could be obtained by solving the chemical reaction-diffusion equations, knowing the pitch variation with concentration (work underway, supplementary material S4).

However, the beauty of this system relies on the crucial detail that both HPMC-OH and HPMC-$OCOCF_3$ form cholesteric phases, with vivid reflection colours, in the presence of TFA, and that TFA can diffuse faster than the polymer molecules, dictating a necessary condition for the existence of an instability in the system.

Conclusions

Diffusion of the "reactive solvent", TFA, to the periphery of the samples prepared from HPMC/TFA lyotropic system starts an unusual evolution of the structural colours in the system. The continuously diffusion of the TFA, from the centre to the periphery, drives the system out of the chemical equilibrium. The formation of a rich phase of the ester, at the border, is fed by a rich phase of the ether existing at the centre of the sample (transportation of A molecules by TFA from the centre to the periphery).

This work makes in evidence that diffusion/reaction mechanisms can be responsible for the appearance/disappearance of sequences of structural colours obtained from cellulosic lyotropic solutions, in the presence of "reactive solvents". In this case the strong acid, TFA, sets in the process, which is a consequence of its diffusion in the medium, and its role as a reactant, and as an auto-catalyst for the chemical reaction. The results obtained suggest the possibility of using diffusion-reaction gradient models[8, 9, 34] to explain the emergence of structural colours in certain cellulosic systems. The work involving the simulation of the patterns, observed for this system, is underway.

There are no conflicts to declare

Acknowledgements

This work is funded by FEDER funds through the COMPETE 2020 Program, National Funds through FCT - Portuguese Foundation for Science and Technology and POR Lisboa2020, under the projects numbers POCI- 01-0145-FEDER-007688 (Reference UID/CTM/50025), UID/BIA/00329/2013, PTDC/CTM-BIO/6178/2014, M-ERA-NET2/0007/2016 (CellColor), PTDC/CTM-REF/30529/2017 (NanoCell2SEC), Action European Topology Interdisciplinary Action (EUTOPIA CA17139) and Slovenian Research Agency Grant Z1-5441 & Programme P1-0099.

References

1. R. D. Deegan, O. Bakajin, T. F. Dupont, G. Huber, S. R. Nagel, T. A. Witten, *Nature*, 1997, **389**, 827-829.
2. X. Mu, D. G. Gray, *Cellulose*, 2015, **22**, 1103-1107.
3. A. Ghasemi, B. Ahmet Tuna, X. Li, *Scientific Reports*, 2019, **9**:6784.
4. D. G. Gray, *Phil. Trans. R. Soc. A*, 2018, **76**:20170038.
5. S. Kinoshita, S. Yoshioka, J. Miyazaki, *Rep. Prog. Phys.*, 2008, **71**, 076401 (30pp).
6. M. Mishra, *Current Science*, 2014, **107**(2), 186-188.
7. B. D. Wilts, V. Saranathan, *Small*, 2018, **14**, 1802328.
8. R. O. Prum, S. Williamson, *Proc. R. Soc. London, Ser. B*, 2002, **269**, 781-792.
9. H. F. Nijhout, Proc. R. Soc. B., 1990, 239, 81-113.

10. S. Caveney, *Proc. R. Soc. Lond. B*,1971, **178**, 205-225.
11. D. J. Brink, N. G. van der Berg, L. C. Prinsloo, I. J. Hodgkinson, *J. Phys. D: Appl. Phys.*, 2007, **40**, 2189-2196.
12. R. S, Werbowyj, D. G. Gray, *Macromolecules*, 1980, **13**, 69-73.
13. S. -L Tseng, A. Valente, D. G. Gray, *Macromolecules*, 1981, **14**, 715-719.
14. S. -L. Tseng, G. V. Laivins, D. G. Gray, *Macromolecules*, 1982, **15**, 1262-1264.
15. R. S. Werbowyj, D. G. Gray, *Macromolecules*, 1984, **17**, 1512-1520.
16. A. M. Ritcey, D. G. Gray, *Macromolecules*, 1988, **21**, 1251-1255.
17. A. M. Ritcey, K. R. Holme, D. G. Gray, *Macromolecules*, 1988, **21**, 2914-2917.
18. J.- X. Guo, D. G. Gray, *Macromolecules*, 1989, **22**, 2086-2090.
19. I. Rusig, M. H. Godinho, L. Varichon, P. Sixou, J. Dedier, C. Filliatre, A. F. Martins, *Journal of Polymer Science: Part B: Polymer Physics*, 1994, **32**, 1907-1914.
20. T.- A. Yamagishi, F. Guittard, M. H. Godinho, A. F. Martins, A. Cambon, P. Sixou, *Polymer Bulletin*, 1994, **32**, 47-54.
21. K. Miyagi, Y. Teramoto, *J. Mater. Chem. C*, 2018, **6**, 1370-1376.
22. K. Hayata, S. Furumi, *Polymers*, 2019, **11**, 1696 (1-8).
23. G. V. Laivins, D. G. Gray, *Macromolecules*, 1985, **18**, 1746-1752.
24. T. Yamagishi, T. Fukuda, T. Miyamoto, T. Ichizuka, J. Watanabe, *Liquid Crystals*, 1990, **7**, 155-161.
25. J.- X. Guo, D. G. Gray, *Journal of Polymer Science: Part B: Polymer Physics*, 1994, **32**, 2529-2537.
26. G. V. Laivins, D. G. Gray, *Polymer*, 1985, **26**, 1435-1442.
27. S. Suto, S. Kimura, M. Karasawa, *Journal of Applied Polymer Science*, 1987, **33**, 3019-3036.
28. H. Ishii, K. Sugimura, Y. Nishio, *Cellulose*, 2019, **26**, 399-412.
29. K. Cantrell, M. M. Erenas, I. de Orbe-Payá, L. F. Capitán-Vallvey, *Anal. Chem.*, 2010, **82**(2), 531-542.
30. H. Weller, M. Westneat, *PeerJ*, 2019, **7,** :e6398 DOI 10.7717/peerj.6398.
31. H. de Vries, *Acta Cryst.*, 1951, **4**, 219-226.
32. H.- L. Liang, M. M. Bay, R. Vadrucci, C. H. Barty-King, J. Peng, J. J. Baumberg, M. F. L. De Volder, S. Vignolini, *Nature Communications*, 2018, **9**, 4632-4639.
33. P. Pieranski, Cristaux Liquides Lyotropes (private communication).
34. A.M. Turing, *Philos. Trans. R. Soc. Lond. Ser. B Biol. Sci.*, 1952, **237**, 37-72.

Supplementary Material (file annexed and .gif animations)

View Article Online
DOI: 10.1039/D0FD00020E